Scientific Research and Essays Vol. 7(22), pp. 2022-2030, 14 June, 2012
Available online at http://www.academicjournals.org/SRE
DOI: 10.5897/SRE11.2243
ISSN 1992-2248 ©2012 Academic Journals

Full Length Research Paper

Aeromagnetic data interpretation to locate buried faults in Riyadh Region, Saudi Arabia

ElKhedr Ibrahim[1,2]*, Osama Kassem[1] and Abdel Aziz Al Bassam[1]

[1]Saudi Geological Survey Research Chair for Natural Hazards, Department of Geology and Geophysics, College of Science, King Saud University, Riyadh, Kingdom of Saudi Arabia.
[2]Department of Geology, Faculty of Science, Mansoura University, Mansoura, Egypt.

Accepted 30 May, 2012

High resolution aeromagnetic data and various filtered maps are used in the present study to detect buried faults in the Riyadh region, Saudi Arabia. Filtering techniques such as Butterworth filter, tilt derivative, source edge detection (SED) and Euler deconvolution (ED) were used to map the structural lineaments in the study area. In this respect, the interpretation of the magnetic anomaly maps indicates that the area is dissected by a number of deep-seated faults that aligned mainly along north-northwest (NNW) and north-northeast (NNE). The northwest (NW), (northeast (NE), west-northwest (WNW) and east west (EW) trending faults are present as second order. These faults divided the study area into three main zones of variable depth, width and pattern. To the northwest, there is an elongated high magnetic anomaly that indicates possible basement uplift, where a wide low magnetic anomaly dominates the western side of the area, with three local and circular low magnetic anomalies. This anomaly pattern is interpreted as a large and regional basinal area with three local depocenters seperated by structural uplifts. The southwestern corner of the area is characterized by a general shallow basement structure with local low magnetic anomalies that form the Awsat and Nisah grabens. The edges of the interpreted structural zones are delineated clearly using SED techniques and the average depth to the magnetic sources ranged from ~5300 to ~ 1300 m.

Key words: Aeromagnetic data, basement structures, faults, Riyadh region, Saudi Arabia.

INTRODUCTION

The area under investigation is Riyadh region, bounded by latitudes 24° and 25° N and longitudes 46.5° and 48° E (Figure 1). This area lies in the eastern part of the Najd province in the east-central part of Saudi Arabia. Riyadh and its suburban areas occupy most of the region, especially the northwest corner. The urban development in and around Riyadh makes the demand of subsurface information an essential issue, especially faults and related structures.

Aeromagnetic data has been widely used to map and delineate the spatial distribution and locations of the structural faults that affect the crystalline basement rocks and overlying sedimentary section. As a general rule, the magnetic anomaly is governed by the contrast in the magnetic susceptibility between the crystalline basement rocks and overlying Phanerozoic cover. In the study area, the Phanerozoic rocks are essentially magnetically transparent (Reynolds et al., 1990; Hudson et al., 1999) and consequently, the magnetic anomaly field in the study area reflects the structure of the Precambrian basement. Therefore, this method is useful for mapping faults that offset basin fill and for delineating near surface buried igneous bodies (Grauch, 2001).

High-resolution aeromagnetic data is used here as a basis for mapping and interpretation of the shallow and deep fault architecture in the study area. The study area was flown by Geosurvey International Ltd. for the Saudi Geological Survey during 1982 to 1983 with altitude of 120 m and flight line direction of N90°E and traverse spacing of 2000 m using Geometrics G813 Proton precession magnetometer with digital recording. As a first step, the total-field magnetic line data was gridded using

*Corresponding author: E-mail: eibrahim@ksu.edu.sa.

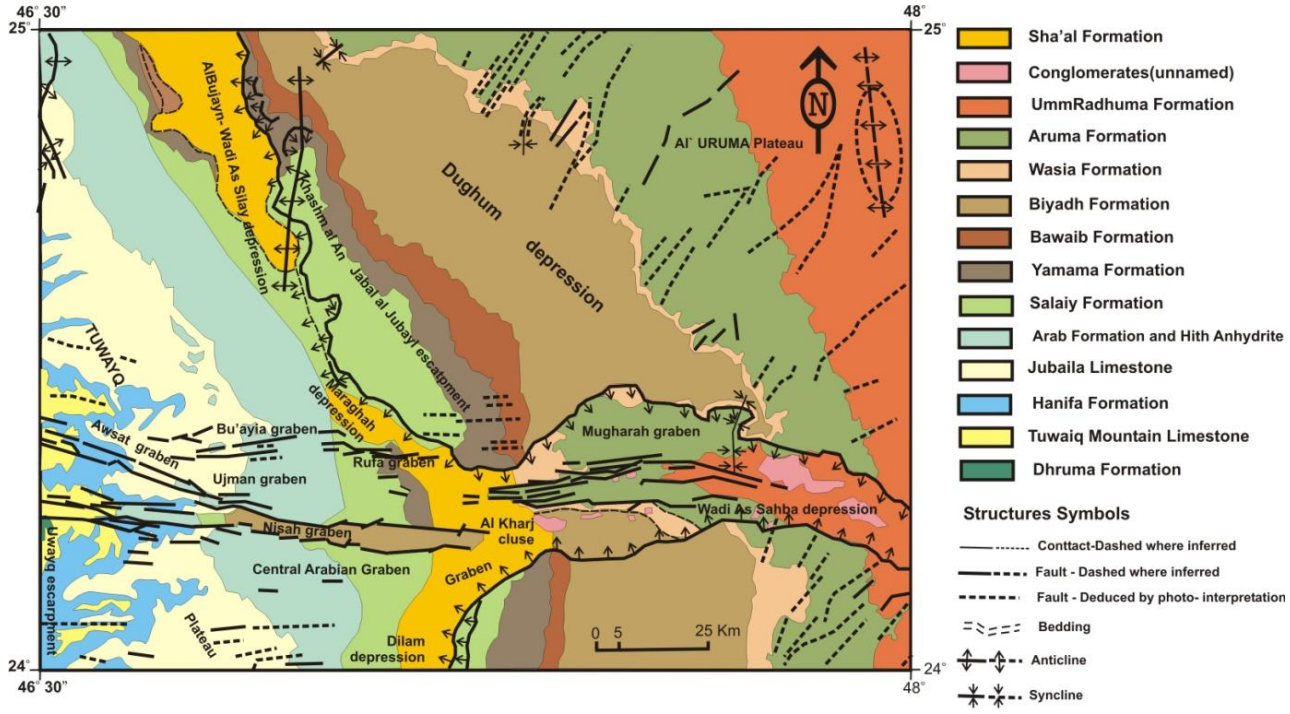

Figure 1. Geological map of Riyadh Region (adapted after Veslet et al., 1991).

a minimum curvature routine approximately one-fourth of the line spacing of the survey using Oasis Montaj software package to get the total field magnetic intensity map.

GEOLOGIC OVERVIEW

The geological map of the study area (Figure 1) shows that the entire Riyadh area is covered with Phanerozoic sedimentary rocks of the western edge of the Arabian platform, which rests on Proterozoic basement at depths estimated between 5 and 8 km (Phoenix Corporation, 1985). The Phanerozoic succession is unconformably overlain in much of the area by Late Tertiary to Quaternary eolian, fluviatile, and (lacustrine) depression deposits. The area is structurally dissected by different sets of faults into grabens and horsts (Figure 1). Powers et al. (1966) proposed that faulting in the central Arabian graben and trough system began in the Late-Cretaceous time and may have continued until the Eocene. Graben boundaries are defined by high-angle normal faults commonly cutting the steep limbs of associated inward-facing monoclinal flexure zones. Trough margins are defined by inward-facing monoclinal flexures locally accompanied by subsidiary normal faults. The Awsat and Nisah grabens are compound structures and consist of two overlapping segments. The three large troughs are Bu'ayja, Mugharah, and Sahba-Mugharah trough and the Maraghah monocline defined as separate structures (Figure 1). Fault zones along graben margins commonly comprise a principal boundary fault, subsidiary antithetic or synthetic normal faults, and minor antithetic or synthetic extension faults, that is, small faults that result in layer-parallel elongation.

MATERIALS AND METHODS

In order to achieve the main objective of the study, special filters are used to enhance the aeromagnetic signature and linear aeromagnetic anomalies and get a clear view of buried faults from the aeromagnetic data. The used total magnetic intensity (TMI) data are corrected for IGRF and the coordinates were also converted to the WGS84 spheroid using the Ain el Abd (1970) datum. This basic dataset (TMI) is uncorrected for the inclination of the Earth's magnetic field and hence anomalies are typically manifested as a magnetic maximum to the south of the causative body, with a minimum to the north. In order to place anomalies directly above the source, Reduced to the Pole (RTP) was carried out on the total magnetic intensity data (Figure 2). This effectively gives the equivalent anomaly pattern which would be observed at the north magnetic pole where the ambient field is vertical, that is, the dipole (high-low anomaly pair) observed over each source is converted to a single maximum directly over the body. This process simplifies the interpretation of the magnetic anomaly data. In addition, special filters are used in order to condition the data set and to render the resulting presentation in such a way as to make it easier to interpret the significance of anomalies in terms of their geological sources. However, a common filtering technique consists into the separation of long (deep) and short (shallow) wavelength anomalies. The cut-off wavelengths and information about the contribution of the short and long wavelengths in the spectrum can be obtained from the calculated radially-averaged power spectrum (Figure 3) of the data. The RTP data was separated into regional and residual compo-nents through application of the Butterworth filtering technique.

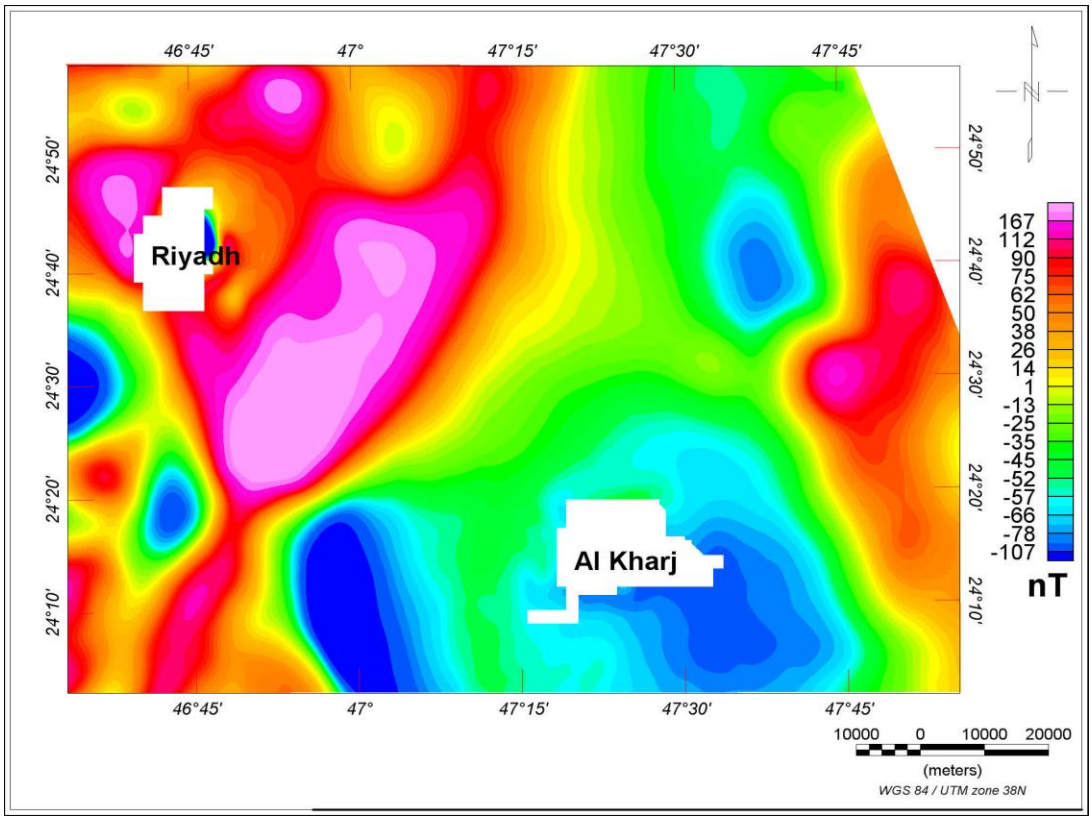

Figure 2. Reduced to the Pole (RTP) magnetic map.

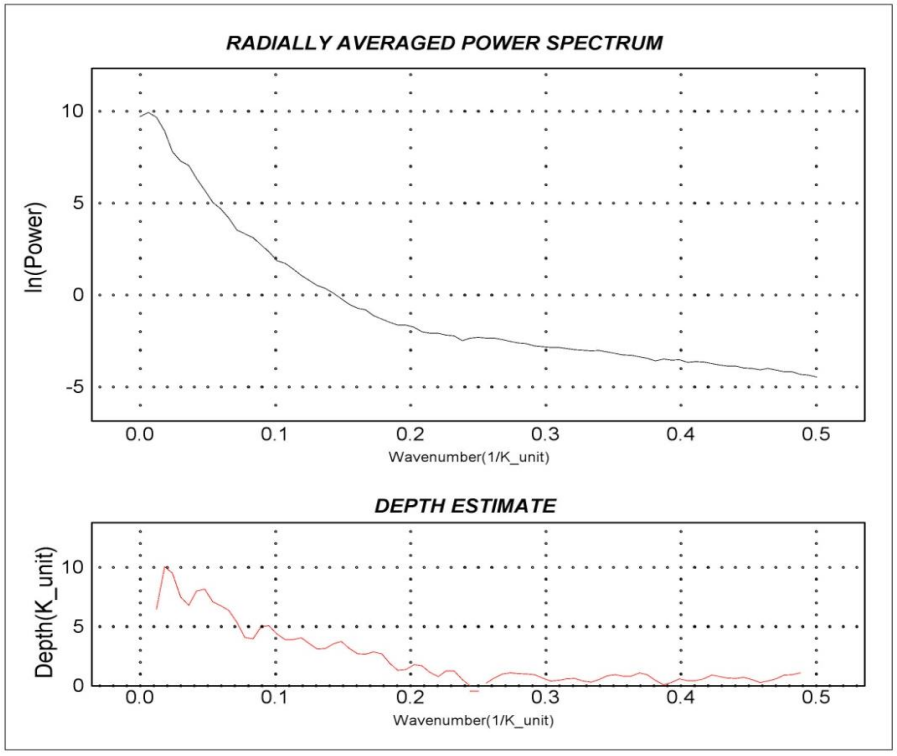

Figure 3. The calculated radially-averaged power spectrum of the magnetic data.

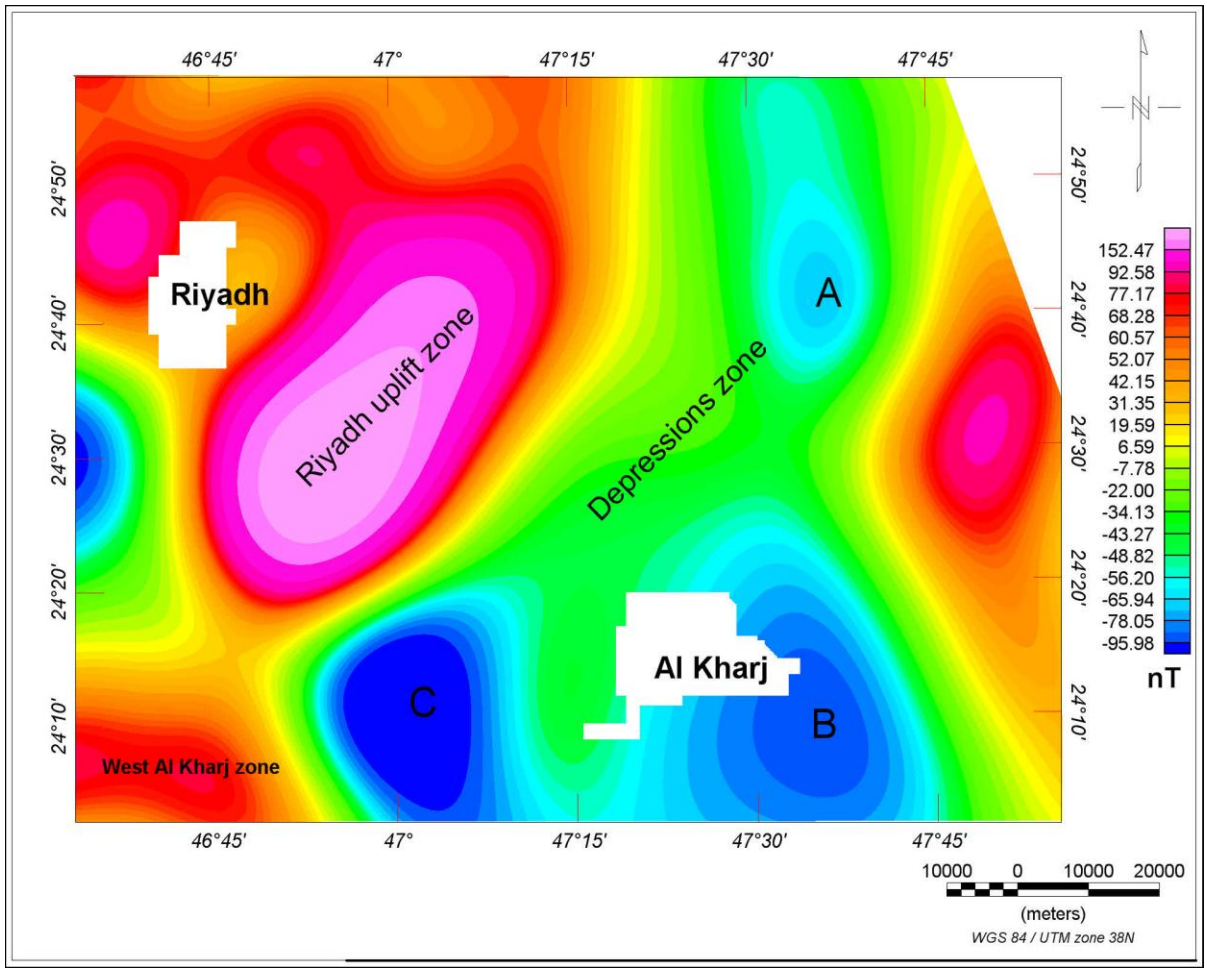

Figure 4. The regional magnetic anomaly map obtained by applying the Butterworth filter technique and the interpreted structural zones.

The regional (Figure 4) and residual (Figure 6) magnetic anomaly maps are obtained by applying frequency domain filters of which the Butterworth filter for high and low cut frequency is applied. This filter is preferably used in the present study rather than the band-pass or high-low pass filters to overcome the ringing effects (Pawlowski and Hansen, 1990).

In this study automatic interpretation techniques were applied to delineate the structures from the RTP magnetic anomaly data. The general requirement for automatic lineament detection algorithm is the transformation of the data such that the edge of a causative body is located beneath a maximum in the grid. Several automatic interpretation techniques satisfy this requirement e.g. source edge detection (SED) and Euler deconvolution (ED). The advantage of the horizontal gradient (HG) method is the low susceptibility to the noise and robustness in delineating either shallow or deep structures (Phillips, 1998). The SED technique extends the horizontal gradient method to locate the peaks in the horizontal gradient grid and defines the source boundaries in vector format (that is, define its strike and dip). In this respect, tilt derivative that is based on the ratio of the first vertical gradient (FVD) and the total HG of the field (Miller and Singh, 1994) is used to depict the edges of deep and shallow magnetic sources. In addition, the TDX (arctan (total_HG /FVD) grid which is calculated from the input total HG and FVD grids and the positive peak values in TDX grid are then extracted to locate the source edges (Figure 5). Euler deconvolution (Reid et al., 1990) is an automatic technique used for locating the source of potential field based on both their amplitudes and gradients. Local wavenumber (SPI) method (Smith et al., 1998) is a technique based on the extension of complex analytical signal to estimate magnetic depths. The main advantage of this method is that the interference of anomaly features is reducible, since the method uses the second-order derivatives. The peaks of SPI functions were traced by passing a small 3 by 3 window over the grid data and searching for maxima (Blakely and Simpson, 1986).

DISCUSSION AND INTERPRETATION

As a general rule, the magnetic anomaly is governed by the contrast in the magnetic susceptibility between the crystalline basement rocks and overlying Phanerozoic cover. The Phanerozoic sedimentary cover of the study area, mainly formed by carbonate rocks belonging to the Arabian platform, is magnetically transparent and does not generate regional-scale magnetic anomalies. Consequently, the magnetic anomalies in the study area reflect

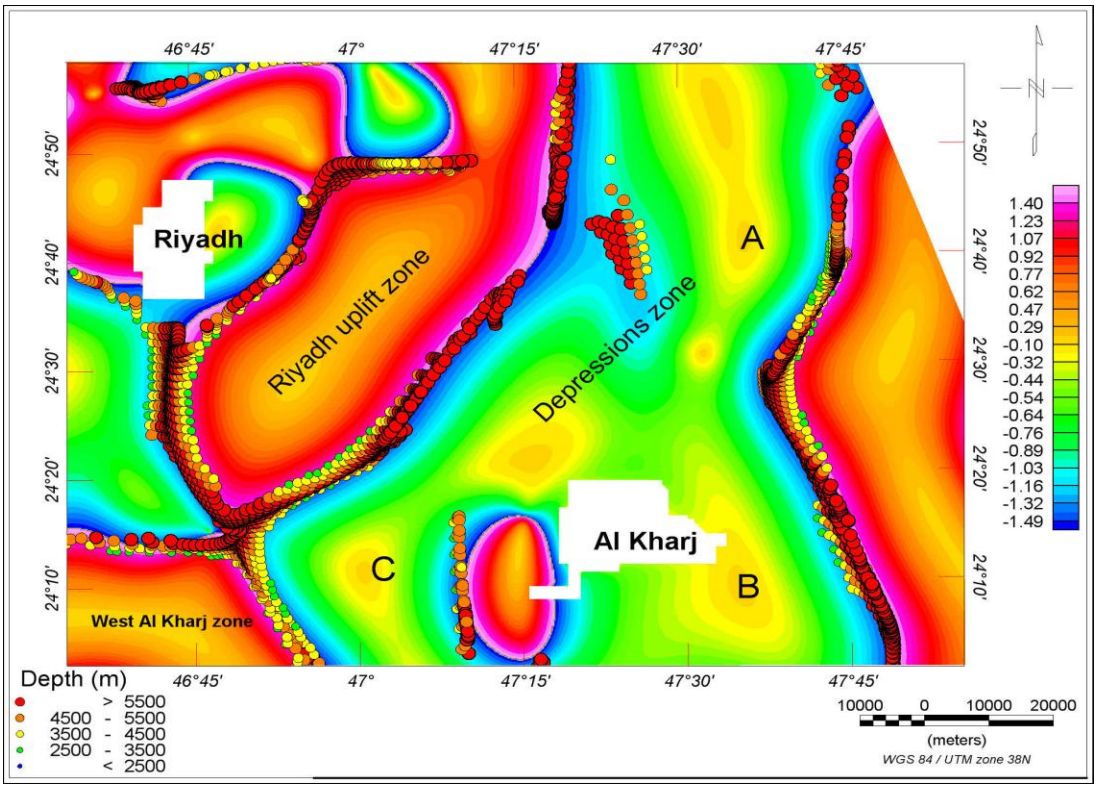

Figure 5. Tilt derivative map overlain by Euler solutions (SI=0.0) for the regional filtered magnetic map.

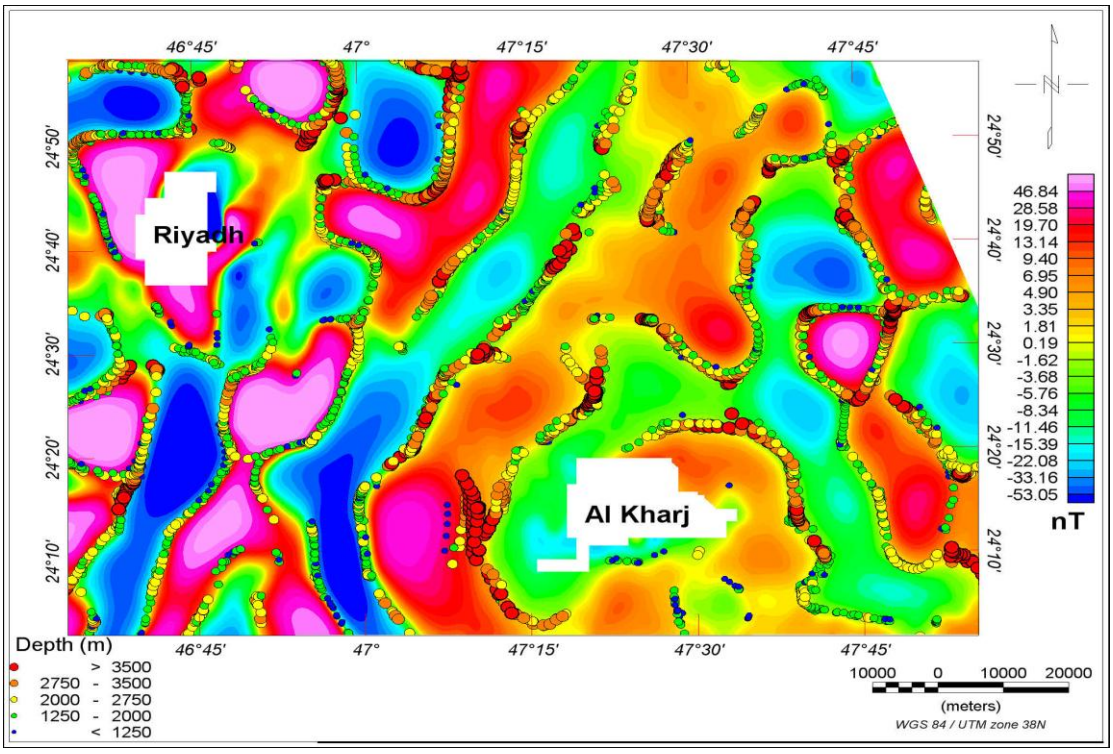

Figure 6. The residual magnetic anomaly map obtained by applying the Butterworth filter technique overlain by Euler solutions (SI=0.0).

the structure of the Precambrian basement. In this study high-resolution aeromagnetic anomalies allow discrimination of many linear features that commonly correspond with geologically concealed faults (e.g. Mogren et al., 2011; Grauch, 2001; Hudson et al., 1999) that are interpreted from a combination of offsets and truncations of magnetic anomalies, and steep gradients in the magnetic data.

The RTP map (Figure 2) indicates that the major magnetic anomaly patterns are aligned mainly along the NNW, NNE, NW, NE, WNW and EW directions and there is a general decrease in the magnetic relief eastward with some exceptions of small narrow and local high magnetic anomalies. Based on the anomaly patterns and magnetic anomaly trends of the regional magnetic anomaly map (Figure 4) and tilt derivative maps (Figure 5), the study region can be divided into three main magnetic anomaly zones. The northwestern zone (Riyadh zone) is dominated by high a magnetic anomaly and is correlated to shallow basement or horst basement structure. This zone is dissected by NW and NE trending faults and is bounded from the eastern side by NNW Najd trending fault that forms the eastern side of the escarpment of Gabel Tuwaiq that is capped by the Tuwaiq Mountain Limestone. The western zone (depressions zone) which is characterized by a relatively broad low magnetic anomaly that separated from the Riyadh uplifted zone by steep magnetic anomalies trending mainly in the NE direction indicating abrupt change in depth caused by faulting, where its eastern side is characterized by an elongated high magnetic anomaly that is related to uplifted basement beneath Al-Uruma plateau. Based on the pattern and amplitude of the regional magnetic anomalies (Figure 4), this zone comprises of three local depocenters (A, B and C) that are occupied by the Dughum, Mugharah and Dilam depressions, respectively. The first two depocenters (A and B) are separated by WNW trending uplift where the depocenters (B and C) are separated by a nearly NS trending uplift.

The third zone (West Al-Kharj zone) is located to the west of Al Kharj town and to the southwestern corner of the study area. This zone is characterized by a relatively a high relief magnetic anomaly on the regional scale (Figure 4) with several closures attaining low amplitude magnetic anomalies superimposed forming discontinuous magnetic anomalies on the local scale (Figure 5). The pattern of the anomaly in this zone could be referred to basement topography and/or shallow prominent uplifted basement structure. This zone is delimited from the east by an elongated low magnetic anomaly that represents the NNW graben of Dilam depression and is dissected by ENE to EW trending faults which form the Awsat and Nisah grabens. The northern Riyadh uplifted zone is separated from this zone by EW trending faults that forms the EW trending grabens that form the passway of Wadi Nisah and its eastern extension of Wadi As Sahba. The edges of these structural zones are depicted using tilt derivative (Figure 5) that is based on the ratio of the vertical gradient and the total horizontal gradient of the field (Miller and Singh, 1994).

The depths of the magnetic sources are estimated using Euler and SPI analysis techniques (Figures 5 to 7) that indicate that the average depth to the magnetic sources ranges from ~5300 to ~ 1300 m (below the flight elevation of 120 m) respectively.

The structural faults that affected the study area are delineated and plotted in Figure 8. This structural analysis indicates that the direction of the faults in the studied area trending occurs mainly in the WNW to ENE and E-W. The rose diagrams (Figure 9a and b) indicate that the value of the faults direction shows clustering along N to ENE and also along N to WNW trends. The average direction for rose and stereographic diagram is 335° indicating that the main faults effected in studied area trend toward NW direction.

The structural analysis indicates that the area is effected by number of faults. The interpreted faults are statistically analyzed in order to determine the main structural trends affected the study area. These faults divided into deep-seated faults and shallow faults. The main and deep trends deduced from the regional magnetic anomaly map (Figure 4) and its rose diagram representation (Figure 9a) indicates that the deep seated faults in the study area are trending mainly in the NE, NW, NNW, WNW to ENE and the average direction is 332° (Figure 9a); while the shalllow weaker trends deduced from residual magnetic anomaly map (Figure 6) and its rose diagram representation (Figure 9b) indicates that the shallow and weaker trends that affect the sedimentary cover rocks in the study area are trended along NE, NNW, NNE with minor EW and NS directions with average direction of about 18° (Figure 9b). The comparison of the shallow and deep tectonic trends indicate that the main trends that mainly dominate and affect the study area is the NE and NNW directions and these faults controlled the formation of sedimentary rocks of the western edge of the Arabian platform as reported before by Johnson and Stewart (1995). Furthermore, the NNW to NW trends represents a system of faults known as the Najd faults direction that cut the Arabian Shield (Moore, 1979).

Conclusions

It is concluded that the study area is dissected by NNW, NNE. The NW, NE, WNW and EW trending faults. These faults divided the study area into three main tectonic zones. The northwestern zone (Riyadh zone) that is characterized by shallow basement structure that dissected by NW and NE trending faults and is bounded from the eastern side by NNW Najd trending fault that forms the eastern side of the escarpment of Gabel Tuwaiq. The western zone (depressions zone) which is

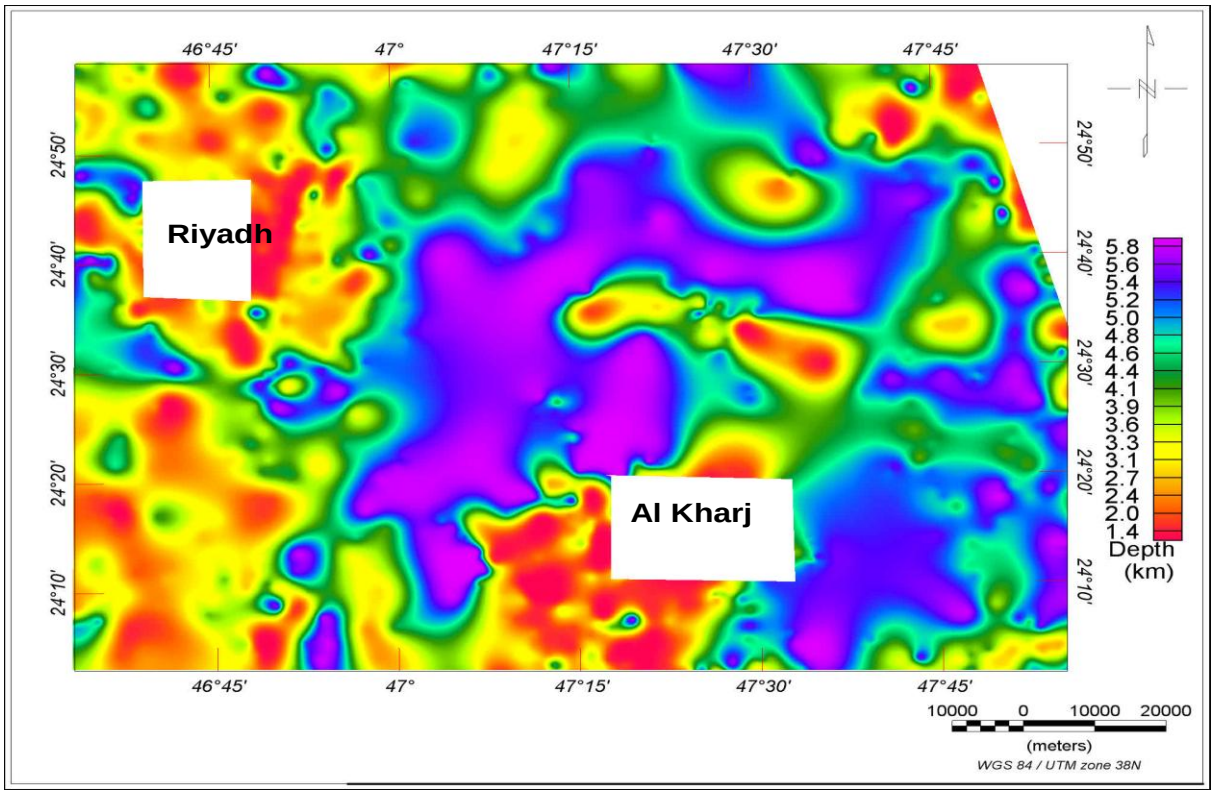

Figure 7. Local wavenumber (SPI) map based on the extension of complex analytical signal to estimate magnetic depths to the basement in the study area.

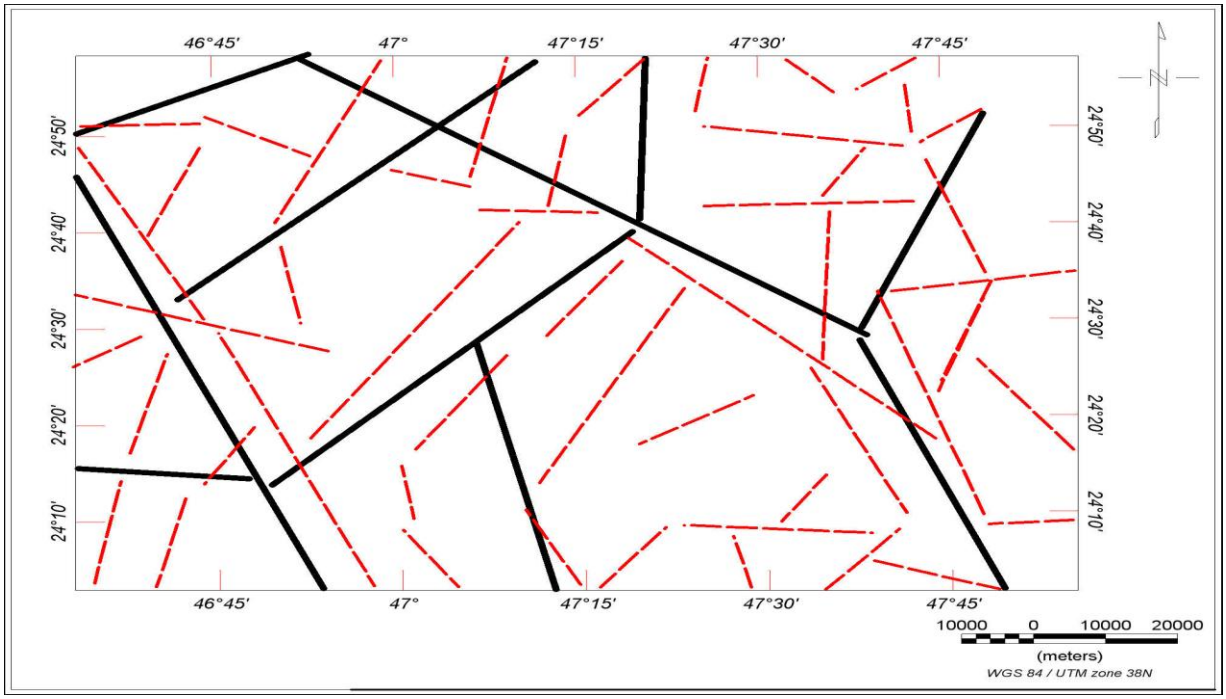

Figure 8. Delineation of the structural faults affected the study area. Heavy black lines = main trends deduced from the regional magnetic anomaly map. Thin dashed red lines = weaker and shallow trends deduced from residual magnetic anomaly map.

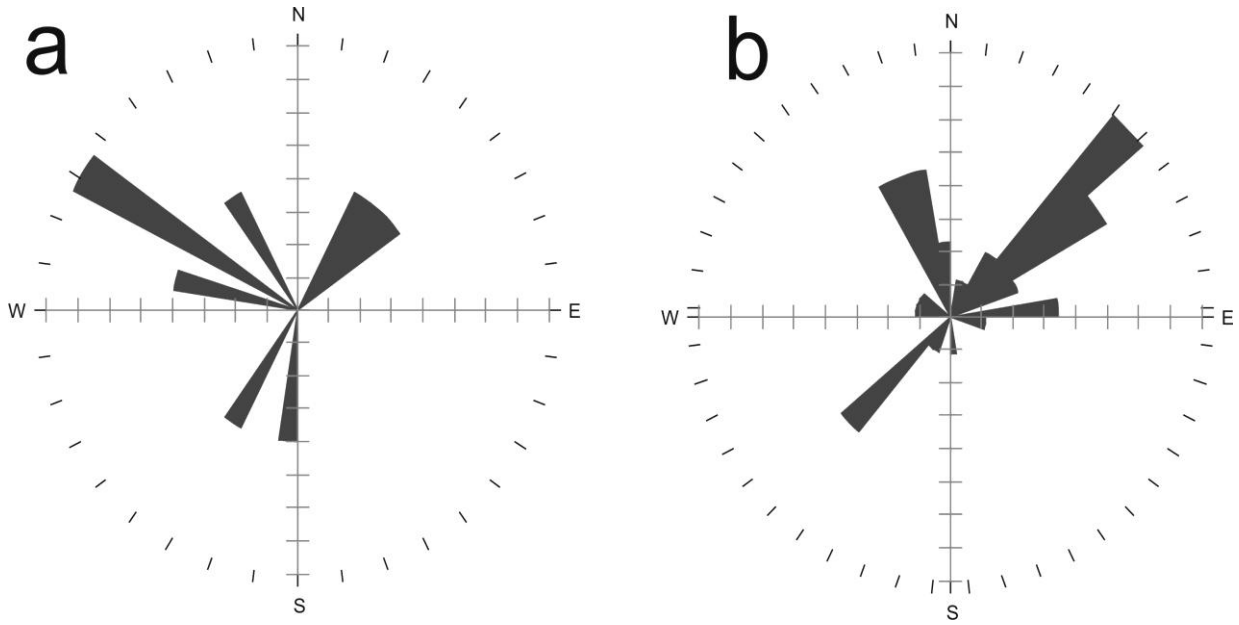

Figure 9. Rose diagram showing (a) the main fault trends deduced from the regional magnetic anomaly map and (b) the weaker (shallow) trends deduced from residual magnetic anomaly map.

separated from the Riyadh uplifted zone by NNE trending fault, where its eastern side is characterized by an elongated high magnetic anomaly that is related to uplifted basement at Al-Uruma plateau. The third zone (West Al-Kharj zone) is located to the southwestern corner of the study area and is characterized by shallow uplifted basement structure. This zone is delimited from the east by an elongated low magnetic anomaly that represents the NNW graben of Dilam depression and is dissected by ENE to EW trending faults which form the Awsat and Nisah grabens. The structural analysis of the interpreted faults indicates that the area is affected by main trends that are directed in the NE and NNW directions and these faults controlled the sedimentary cover of the western edge of the Arabian platform as previously reported by Johnson and Stewart (1995). The edges of these structural zones are delineated clearly using SED techniques and the average depth to the magnetic sources ranges from ~5300 to ~ 1300 m.

ACKNOWLEDGEMENTS

This work was carried out under the Saudi Geological Survey Research Chair for Natural Hazards at the Geology and Geophysics Department in King Saud University, Riyadh, Saudi Arabia.

REFERENCES

Blakely R, Simpson R (1986). Approximating edges of source bodies from magnetic or gravity anomalies. Geophysics, 51: 1494-1498.

Grauch V (2001). Using high-resolution aeromagnetic surveys to map subsurface hydrogeology in sediment-filled basins—A case study over the Rio Grande rift, central New Mexico, USA. Explor. Geophys., 32: 209-213.

Hudson M, Mikolas M, Geissman J, Allen, B (1999). Paleomagnetic and rock magnetic properties of Santa Fe Group sediments in the 98th Street core hole and correlative surface exposures, Albuquerque Basin, New Mexico. New Mexico Geological Society 50th field conference, Albuquerque Basin, Guidebook, pp. 355-361.

Johnson PR, Stewart ICF (1995). Magnetically inferred basement structure in central Saudi Arabia. Tectonophysics, 245: 37-52.

Miller H, Singh V (1994). Potential field tilt—a new concept for location of potential field sources. J. Appl. Geophy., 32 (2-3): 213-217.

Mogren S, Batayneh A, Elawadi E, Al-Bassam A, Ibrahim E, Qaisy S (2011). Aquifer boundaries explored by geoelectrical measurements in the Red Sea coastal plain of Jazan area, Southwest Saudi Arabia. Int. J. Phys. Sci., 6(15): 3768-3776.

Moore JM (1979). Tectonics of the Najd transcurrent fault system, Saudi Arabia. J. Geol. Soc. London, 136: 441-454.

Pawlowski R, Hansen R (1990). Gravity anomaly separation by Wiener filtering. Geophysics, 55: 539-548.

Phoenix Corporation (1985). The interpretation of an aeromagnetic survey of the cover rocks region, Kingdom of Saudi Arabia. Saudi Arabian Deputy Ministry for Mineral Resources DMMR, unnumbered report.

Phillips J (1998). Processing and Interpretation of Aeromagnetic Data for the Santa Cruz Basin-Patahonia Mountains Area, South-Central Arizona. U.S. Geological Survey Open-File Report, pp. 2-98.

Powers R, Ramirez L, Redmond C, Elbererg E (1966). Geology of the Arabian Peninsula: sedimentary geology of Saudi Arabia. U. S. Geol. Surv. Prof. Pap., 560-D: 147.

Reid A, Allsop J, Granser H, Millett A, Somerton WI (1990). Magnetic interpretations in three dimensions using Euler deconvolution. Geophysics, 55: 80-91.

Reynolds R, Rosenbaum J, Hudson M, Fishman N (1990). Rock magnetism, the distribution of magnetic minerals in the Earth's crust, and aeromagnetic anomalies. U.S. Geol. Surv. Bullet., 1924: 24-45.

Smith R, Thurston J, Dai T, and MacLeod I (1998): ISPI - the improved source parameter imaging method. Geophys. Prospect., 46: 141-151.

Vaslet D, Muallem M, Brosse J, Fournieuet J, Breton J, Le Nindre Y

(1991). Geologic map of the Ar Riyad Quadrangle, Sheet 24 I. Kingdom of Saudi Arabia, Saudi Arabian Deputy Ministry for Mineral Resources (DGMR) Geoscience Map GM-121 C, scale 1: 250000.